

Nighttime Photovoltaic Cells: Electrical Power Generation by Optically Coupling with Deep Space

Tristan Deppe^{†,‡} and Jeremy N. Munday^{*,†,‡,§} 

[†]Department of Electrical and Computer Engineering and [‡]Institute for Research in Electronics and Applied Physics, University of Maryland, College Park, Maryland 20742, United States

[§]Department of Electrical and Computer Engineering, University of California, Davis, California 95616, United States

ABSTRACT: Photovoltaics possess significant potential due to the abundance of solar power incident on earth; however, they can only generate electricity during daylight hours. In order to produce electrical power after the sun has set, we consider an alternative photovoltaic concept that uses the earth as a heat source and the night sky as a heat sink, resulting in a “nighttime photovoltaic cell” that employs thermoradiative photovoltaics and concepts from the advancing field of radiative cooling. In this Perspective, we discuss the principles of thermoradiative photovoltaics, the theoretical limits of applying this concept to coupling with deep space, the potential of advanced radiative cooling techniques to enhance their performance, and a discussion of the practical limits, scalability, and integrability of this nighttime photovoltaic concept.

KEYWORDS: sustainable energy, thermoradiative, photovoltaics, radiative cooling, emissive energy harvester, atmospheric transparency window



Currently, over 100 U.S. cities have committed to using 100% clean, renewable electricity by 2050, and solar energy is expected to help supply the needed additional power. However, conventional photovoltaic (PV) cells can only generate electricity during daylight hours. The lack of nighttime performance necessitates the need for costly batteries and grid connection to other sources of energy, most notably fossil fuels. To continue the global push toward carbon neutrality, new sustainable power generation techniques must be employed at night as well. Here we propose an alternative PV concept that employs thermoradiative cells and the advancing field of radiative cooling in order to generate electrical power during the day and throughout the night.

Though the power conversion process of a solar cell is governed by the principle of detailed balance,¹ it can also be modeled as a simplified heat engine. Ultimately the cell delivers power because the radiation source, the sun, is very hot, and the solar cell, in comparison, is cool (Figure 1a). Alternatively, we can heat up the solar cell, which becomes the hot object, and point it at a cold object, for example, the night sky (Figure 1b). In both cases, we have one hot object and one cold object, and we can study the power flow between them. In the second case, this type of heat engine is called a thermoradiative (TR) cell.² Explained in detail in the next section of this Perspective, a TR cell generates power because the emission of thermal radiation from the cell exceeds the absorption of irradiation from the surroundings during operation. The actual devices, a solar cell and a TR cell, are nearly identical; however, the operating currents and voltages have opposite signs because

the radiative processes are reciprocal (Figure 1c). In practice, TR cells can be used as waste heat recovery units in order to extract power from a hot source, for example, an engine's exhaust pipe, a generator's cooling towers, or other heat sources in industrial manufacturing plants. The cell simply needs to be at a higher temperature than the object toward which it radiates. The nighttime PV cell concept relies on the thermoradiative effect and uses the warmth of the earth, at about 300 K, as a heat source and the darkness of space, at 3 K, as a heat sink. The key to making this concept work is then twofold. First, we must choose a material with the appropriate bandgap needed to maximize power output. Second, the device must be able to “see” through the atmosphere in order to optically couple with space.

Regarding bandgap, a typical single junction solar cell is made from a semiconductor with a bandgap in the range of 1–1.5 eV. Most modern commercial cells operate at approximately 20% efficiency and are made of silicon, with a 1.1 eV bandgap, yielding approximately 200 W/m² under peak solar irradiance (~1000 W/m²). If silicon were used for a nighttime PV cell, the principles of detailed balance, outlined in the following section, lead to a maximum power output of $<2 \times 10^{-14}$ W/m². This result is because the photons emitted by a blackbody near room temperature are infrared, with energy far

Received: May 8, 2019

Revised: November 20, 2019

Accepted: November 20, 2019

Published: November 20, 2019

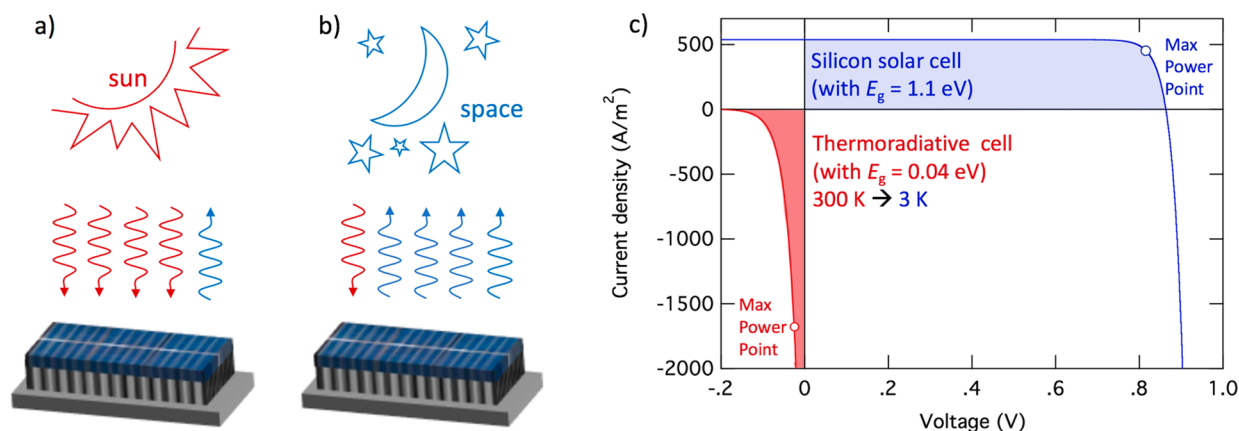


Figure 1. (a) Photovoltaic cell illuminated by solar irradiation during the day. Absorbed photons create electron–hole pairs across the semiconductor bandgap and establish a working voltage, V . (b) Thermoradiative cell at night. The cell emits thermal radiation in the infrared into space. As electron–hole pairs recombine across the semiconductor bandgap, a negative voltage is established. (c) I – V characteristics of a photovoltaic (quadrant 1) and an ideal thermoradiative (quadrant 3) cell of bandgaps 1.1 and 0.04 eV, respectively, both show power generation. For the thermoradiative cell, negative voltage, and negative current generate positive power across an external load.

less than the bandgap of silicon. However, if an ultralow-bandgap material were used to make a device, low energy photon emission results from carrier recombination across the gap and, when connected to a load, an ideal cell could produce as much as 54 W/m^2 under ideal conditions and potentially more than 10 W/m^2 under typical sky conditions, both to be discussed later, without the need for solar absorption (Figure 2). Though this power output is lower than a conventional

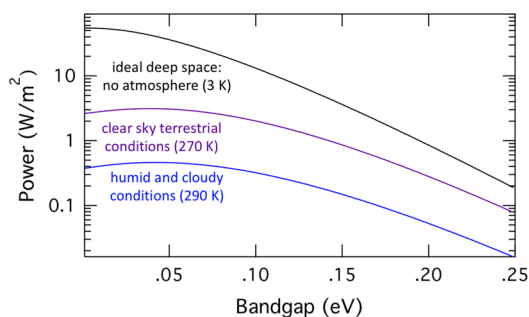


Figure 2. Maximum power density vs bandgap energy for a 300 K terrestrial cell and three selected sky conditions, modeled with effective sky temperatures. The ideal case is a cell directly accessing the darkness of space at 3 K, 270 K simulates clear terrestrial conditions, extrapolated from maximum radiative cooling estimates,^{22,23} and 290 K corresponds to humid and overcast conditions.

solar cell, it could be produced day and night. Further, one can envision a tandem system consisting of a TR device operating at night and a standard solar cell operating during the day to produce higher total around-the-clock power. For example, in an average U.S. climate, such as Boulder, CO, the National Renewable Energy Laboratory database records an average solar irradiance of about 5 kWh/m^2 per day,³ of which a commercial solar cell could harvest 1 kWh/m^2 . A nighttime PV cell in this climate could produce an average of 120 Wh/m^2 (if operated during only 12 h), adding $\sim 12\%$ more power to the 24 h cycle.

To directly access deep space as a thermal reservoir, we next consider the topic of radiative cooling. For millennia humans have understood that material choice and architectural design can heat or cool structures above or below ambient air

temperature.⁴ Today, white paint is sometimes used to coat roofs of buildings in order to reflect sunlight and thereby reduce heating during the day. In recent years, however, the study of radiative cooling has garnered attention with the development of highly thermally emissive, yet solar reflective, materials that can be used to lower an object's surface temperature significantly below ambient.^{5–8} A similar technique can also be extended to traditional solar cells to avoid heating during operation.^{9,10} By appending a photonic material that is visibly transparent yet thermally emissive within the atmospheric transparency window of $8\text{--}13 \mu\text{m}$, solar radiation is still delivered to the cell to generate power, but thermal heat is radiatively exhausted to deep space. These concepts inspire the engineering of a nighttime PV cell in order to extract electrical power from the radiative emission of thermal wavelengths from a device on earth to outer space.

In this Perspective, we first discuss the background and history of thermoradiative photovoltaics and the use of selectively emissive materials in cooling applications. Next, we introduce a simple model for a TR PV device that generates power by using the heat of the earth as a thermal power source and the night sky as a radiative heat sink. We then calculate the fundamental limits of such a device and discuss possible materials, their respective practical limits, and finally, the scalability, integrability, and energy harvesting potential of a nighttime PV cell.

■ THERMORADIATIVE PHOTOVOLTAICS

The physical principles governing TR cells are similar to those behind conventional photovoltaics.^{2,11–14} When a p – n junction is in thermal equilibrium with its surroundings in the dark (Figure 3a), the random absorption of photons by the cell equals the random emission from the cell, and the Fermi level remains constant throughout the semiconductor. Under illumination and normal PV cell operation (Figure 3b), absorption is greater than emission, and this difference generates photocurrent. Photon absorption increases the total electron and hole carrier density, which increases the quantity np to greater than $n_0p_0 = n_i^2$, the square of the total intrinsic carrier density. This excess carrier generation splits the electron and hole Fermi levels within the junction by an amount $\Delta\mu = qV$, which are then referred to as the quasi-Fermi

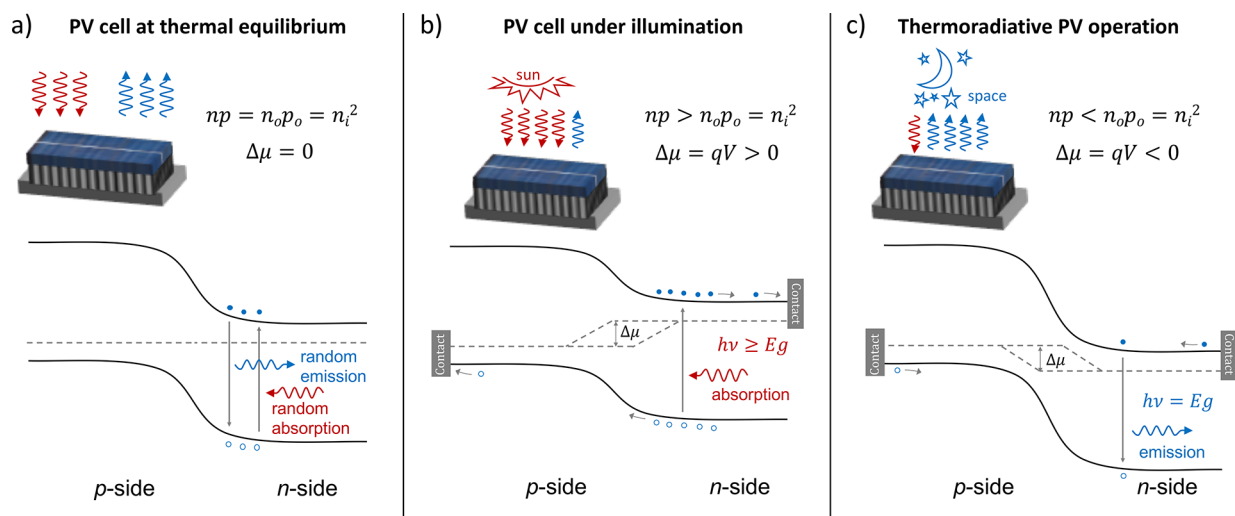


Figure 3. Photovoltaic (PV) cells under different operating conditions, showing band diagrams and the path of carriers through (a) a p - n junction at thermal equilibrium, where emission balances absorption and no current is produced, (b) a p - n junction under illumination, i.e., conventional solar cell operation, where excess carriers are created due to absorption, and (c) a p - n junction functioning as a thermoradiative cell, where emission reduces the carrier concentration below thermal equilibrium, and a reverse bias forms across the junction.

levels. If the cell is connected to a load, excess electrons and holes that do not recombine within the material can be extracted on the n - and p -side, respectively, with energy slightly below qV due to thermodynamic losses. If the p - n junction is at a higher temperature than its surroundings (Figure 3c), emission from the device dominates absorption as the device tries to cool. However, if the cell is connected to a thermal reservoir, its temperature remains constant. In this case, the enhanced emission decreases the carrier concentration below its equilibrium value, $n_0 p_0$, which splits the electron and hole Fermi levels in the opposite direction and introduces a reverse bias voltage across the junction. When short-circuited or connected to a load, the recombination of an electron and hole pair that is not balanced by absorption of a photon results in an additional electron and hole being inserted via the contacts to balance the lost pair. This injection results in current flow. Functionally, the main difference between a TR PV cell and a conventional PV cell is that (i) the current flows in the opposite direction and (ii) the sign of the voltage is also reversed; therefore, both scenarios generate usable power.

To describe the current and power produced by a TR cell at temperature T_c exposed to a cooler body at temperature T_a , we use the principles of detailed balance, formulated by Shockley and Queisser. First, the photon flux emitted from an illuminated or biased semiconductor is derived from Planck's generalized law for blackbody radiation and is equal to¹⁵

$$\dot{N}(T, \Delta\mu) = \frac{2\pi}{h^3 c^2} \int_{E_g}^{\infty} \frac{\varepsilon(E) E^2}{e^{E - \Delta\mu/k_B T} - 1} dE \quad (1)$$

where T , $\Delta\mu$, $\varepsilon(E)$, and E_g are the temperature, the chemical potential driving emission, the energy-dependent emissivity, and the bandgap of the semiconductor, respectively, while h is Planck's constant, k_B is Boltzmann's constant, and c is the speed of light, and the integral is taken over photon energy, E . In the absence of nonradiative recombination, the external current produced by the cell must equal the difference between photon absorption and photon emission. Illuminated by a radiative body at T_a , an ideal cell at temperature T_c will produce a current density through an external circuit equal to

$$J = q[\dot{N}(T_a, 0) - \dot{N}(T_c, \Delta\mu)] \quad (2)$$

where $\Delta\mu_c$ is the cell's chemical potential, which is equal to the quasi-Fermi level splitting and is related to the output voltage by $\Delta\mu_c = qV$. As mentioned above, in a TR cell emission dominates absorption, as $T_c > T_a$. For a cell that is a perfect emitter and absorber of photons at or above the bandgap energy of the semiconductor and is transparent to lower energy photons (i.e., $\varepsilon = 0$ for $E < E_g$ and $\varepsilon = 1$ for $E \geq E_g$), one can see from eqs 1 and 2 that the current will be negative. By attaching a load across the cell, the extractable power density is

$$P = JV = qV[\dot{N}(T_a, 0) - \dot{N}(T_c, qV)] \quad (3)$$

The efficiency of a TR cell has been derived for cases where the devices are heated up to temperatures above ambient^{2,12} and when emission is restricted to a very narrow bandwidth.^{13,14} In our configuration, the cell temperature is maintained at room temperature by the earth and radiates out to space. Because no work is done to heat the cell to $T_c = 300$ K (noting that it is connected to an effectively infinite thermal reservoir), the traditional efficiency, $P_{\text{out}}/P_{\text{in}}$, becomes a less useful metric, as P_{in} is simply conductive sources of heat from the earth and the surroundings plus the ambient radiation into the cell. Thus, the purpose of this manuscript is to analyze the extractable electrical power per unit area rather than the efficiency.

Low bandgap materials are needed for TR devices so that the bandgap energy more closely matches the peak of the device's thermal emission spectrum. In this discussion, we focus on the potential to extract power from a cell around ambient temperature, $T_c = 300$ K, using the Earth as a heat source and the night sky, which also varies in temperature, as a heat sink, as illustrated in Figure 1b. Recently, Santhanam and Fan showed that a HgCdZnTe thermoradiative cell (with $E_g = 0.218$ eV) could deliver 1 pW of power when held at 295 K and exposed to an emissive plate with a 10 K temperature difference.¹⁴ To enhance the extractable power past the pW scale, we consider ideas from the advancing field of radiative cooling to employ deep space as a heat sink to allow for a

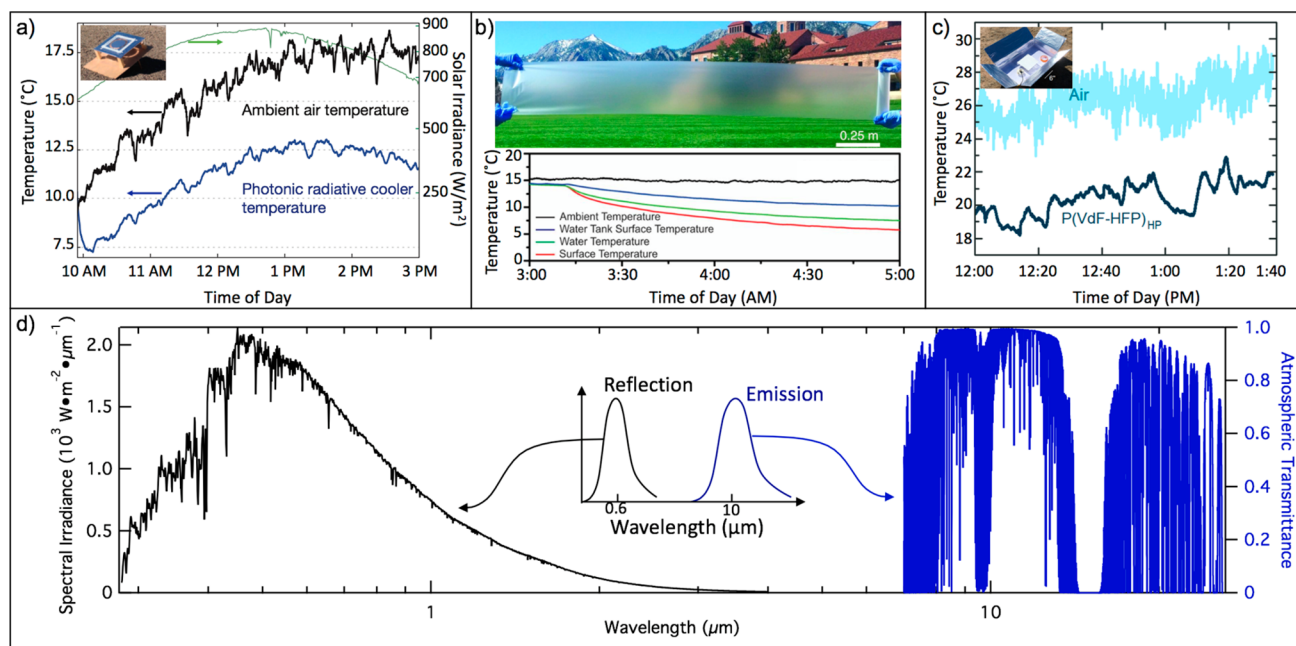


Figure 4. (a) By alternating layers of SiO₂ and HfO₂, Raman et al. demonstrated that a combination of material properties and interference effects will produce a photonic radiative cooler that cools to 4.9 K below ambient air temperature.⁵ (b) Zhai et al. embedded resonant SiO₂ microspheres randomly in a polymethylpentene (TPX) polymer matrix via a roll-to-roll processing method to create a scalable glass-polymer metamaterial that achieves a surface temperature about 9 K below ambient, with notably higher cooling power at night.⁶ (c) Mandal et al. substituted the microspheres for air gaps and produced a scalable phase-inversion based P(VdF-HFP)_{HP} coating that allows for a subambient temperature drop of 6 K.⁸ (d) The majority of the solar irradiance incident on earth (left) falls in the visible range of the electromagnetic spectrum, compared to the transmittance spectrum of the atmosphere (right), of which the portion between 8–13 μm is known as the atmospheric transparency window (ATW). This is the spectral region through which thermal radiation can escape the atmosphere. The inset shows the simplified spectral characteristics of a radiative cooler that reflects the solar wavelengths and emits within the ATW. Image credits: Panel (a) was adapted with permission from Springer Nature Customer Service Center GmbH: Raman, A. P.; Anoma, M. A.; Zhu, L.; Rephaeli, E.; Fan, S. Passive Radiative Cooling below Ambient Air Temperature under Direct Sunlight. *Nature* **2014**, *515* (7528), 540–4. Copyright 2014 Macmillan Publishers Ltd. Panel (b) was adapted with permission from Zhai, Y.; Ma, Y.; David, S. N.; Zhao, D.; Lou, R.; Tan, G.; Yang, R.; Yin, X. Scalable-Manufactured Randomized Glass-Polymer Hybrid Metamaterial for Daytime Radiative Cooling. *Science* **2017**, *355*, 1062–1066. Copyright 2017 AAAS. Panel (c) was adapted with permission from Mandal, J.; Fu, Y.; Overvig, A.; Jia, M.; Sun, K.; Shi, N.; Zhou, H.; Xiao, X.; Yu, N.; Yang, Y. Hierarchically Porous Polymer Coatings for Highly Efficient Passive Daytime Radiative Cooling. *Science* **2018**, *362*, 315–319. Copyright 2018 AAAS.

significantly larger temperature difference and increase power production.

■ RADIATIVE COOLING

The key factors needed for effective radiative cooling are (i) the ability to transmit or reflect solar illumination to avoid heating, (ii) thermal isolation from the environment to limit additional conductive and convective heat exchanges with the surroundings, and (iii) the ability to emit wavelengths that fall within the atmospheric transparency window to enable radiative heat transfer to deep space. While earth's atmosphere absorbs and reflects at various wavelengths, there is a region within the infrared portion of the electromagnetic spectrum for which the atmosphere is mostly transparent. This is known as the atmospheric transparency window (ATW) and falls roughly between 8–13 μm (Figure 4d). Note there is also a secondary window at slightly longer wavelengths. The earth, whose surface temperatures range from about 220 to 320 K, emits strongly within this infrared window. These long-wave infrared (LWIR) wavelengths can pass through the atmosphere, a phenomenon that allows for the earth to regulate its own temperature and remain habitable. Furthermore, materials that emit and absorb predominately over this bandwidth but reflect or transmit the solar spectrum are optically coupled to deep space but blind to the atmosphere and the sun. Using a

material with such a tailored emission spectrum allows for the dramatic cooling of its substrate through photonic emission both at night and under direct sunlight. This concept has also recently been suggested as an additional mitigation strategy to address climate change.¹⁶

As mentioned previously, white paints have traditionally been used to achieve this effect on a commercial scale as they reflect most of the solar spectrum, with hemispherical solar reflectivity, R_{solar} up to ~0.94 (over a wavelength range of ~0.3–2.5 μm), and emit well in the IR, with broadband hemispherical thermal emittance, ϵ_{IR} up to ~0.90 (over a wavelength range of 3–25 μm).¹⁷ However, common pigments like titania and zinc oxide absorb strongly in the UV, which can limit cooling performance under direct sunlight.^{6,7} Some transparent polymers, such as PMMA,¹⁸ have excellent broadband thermal emittance, while others, like TPX and PVF,¹⁹ emit selectively in the LWIR. Consequently, there are numerous thermoplastic films and membranes available on the market that utilize different combinations of polymers to achieve effective daytime cooling, the best with R_{solar} and ϵ_{IR} around ~0.90.¹⁷ In recent years, rapid advancements in radiative cooling have been made to craft different types of photonic metamaterials, many based on these emissive polymers, that can improve on commercially available paints and films.^{5–8} The materials highlighted in Figure 4a–c

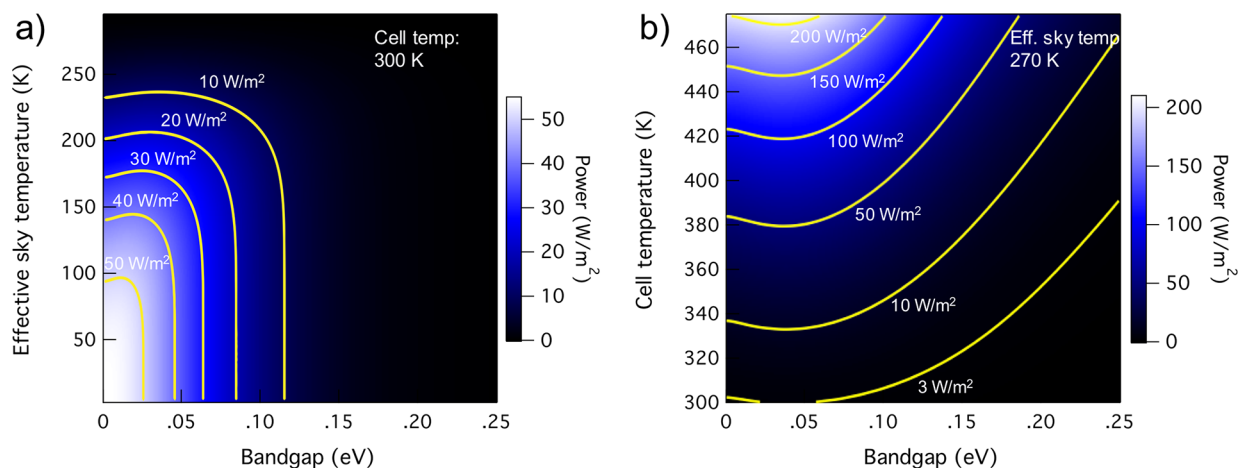


Figure 5. (a) Maximum power output of a thermoradiative cell, held at 300 K, whose semiconductor bandgap ranges from 0 to 0.25 eV for effective sky temperatures 3 to 295 K. The optimal bandgap increases as effective sky temperature increases, showing broadening contour lines. (b) Maximum power output of a thermoradiative cell at a range of temperatures, coupled with the sky at an effective temperature of 270 K, simulating clear sky conditions.^{22,23}

are constructed differently yet operate on similar principles. When appended to other surfaces, these materials have been shown to actually reduce substrate temperature below ambient and, in arid environments, are capable of radiating around 100 W/m² night and day.^{6,8} Metamaterials based on paint-format SiO₂ microspheres,⁷ similar to the method characterized by Gentle and Smith,²⁰ or the porous P(VdF-HFP)_{HP} coating highlighted in Figure 4c, with $R_{\text{solar}} > 0.96$ and hemispherical LWIR emittance of $\epsilon_{\text{LWIR}} > 0.97$, outperform commercial daytime cooling methods while retaining their scalability.

FUNDAMENTAL LIMITS

Before discussing the output potential of a terrestrial nighttime PV device exposed to the sky, we first calculate the general power limits for a TR system by applying the principle of detailed balance outlined previously. We find that an ideal TR cell at 300 K coupled with a 3 K radiating body (deep space) has a maximum power output of 54 W/m². The power output is highest below a bandgap of 0.05 eV (3 K curve of Figure 2). Figure 5a shows the maximum power that can be obtained from a TR cell at $T_c = 300$ K with $0 < E_g \leq 0.25$ eV exposed to a blackbody radiator of temperature $3 \text{ K} \leq T_a \leq 295$ K. We refer to these T_a as effective sky temperatures, which approximate the amount of downwelling (or incident) infrared radiation a terrestrial cell may experience from the atmosphere, space, or another object in the form of a blackbody. While the actual radiation spectrum should be used when available, for simplicity, we model the total downwelling radiation as a blackbody with an effective sky temperature, T_a (see eq 1), where the temperature is chosen to provide the total number of absorbed photons that would be expected from an ambient temperature blackbody with semitransparent emission windows defined from experimental data at different locations and weather conditions. Note that the optimal bandgap trends away from 0 eV as the effective sky temperature increases from 3 K. As effective sky temperature increases, so does the peak of its emission spectrum and, thus, the average number of incident photons on the cell increases. With low bandgap semiconductors, these photons will be increasingly absorbed by the cell, which will decrease the cell's power output, as its own emission does not increase at the same rate. Increasing the bandgap of the semiconductor with the effective sky temper-

ature thus limits the absorption of these increasingly energetic incident photons, and so, the max power point is found at an increasingly higher bandgap. For a TR PV cell at 300 K to produce a useful amount of power, the material bandgap needs to be less than 0.1 eV. While coupling directly with deep space at 3 K is optimal for power conversion, this 54 W/m² target is only obtainable for an extraterrestrial device held at 300 K. Due to the emission spectrum of the atmosphere, for a terrestrial device to directly access the darkness of space, we could restrict its emissivity to only the ATW using a selective emitter; however, this results in a significantly lower maximum power output of 11.8 W/m² (for a material with $E_g = 0.095$ eV), assuming zero emission from the sky within the window, which is however unlikely. To determine the maximum achievable power for a terrestrial cell exposed to the sky, we return to the concept of radiative cooling and a more precise analysis of atmospheric emission.

For optimal subambient cooling under direct sunlight, a radiative cooler would selectively emit only within the ATW with $\epsilon_{\text{LWIR}} \sim 1$ and $\epsilon \sim 0$ elsewhere. However, for a TR device, the intent of the emission is not to cool it down, but rather to ensure it radiates well in the IR to maximize the radiative power. Furthermore, some radiative coolers, like those highlighted in Figure 4a,b, use thin metal layers to reflect incident sunlight for daytime cooling.^{5,6} Note that such a requirement is not necessary for nighttime operation of the TR devices we are considering; however, the sun could also be used to heat the TR material if operating during the day, as discussed below, or the solar illumination could be used by another device (e.g., a traditional solar cell), so long as the semiconductor of the TR cell does not absorb the sunlight. The device should emit strongly over thermal wavelengths, similar to the behavior of the porous polymer material⁸ highlighted in Figure 4c, which happens naturally for the low-bandgap materials required for power production. For operation under direct sunlight (e.g., to enable 24 h power production), we find that R_{solar} as low as 0.5 will allow for the 300 K TR device to produce >1 W/m² power, but the optimal bandgap shifts closer to zero as R_{solar} decreases from unity. There is less restriction, however, on the required thermal emissivity due to the several orders of magnitude difference between absorbed and emitted photons. An ϵ_{IR} of 0.4 will

allow for $>1 \text{ W/m}^2$ power production, and the nighttime PV device will produce power, though negligible ($<0.1 \text{ W/m}^2$), with ε_{IR} as low as 0.01. As stated previously, available materials with $\varepsilon_{\text{IR}} > 0.9$ are common.

To accurately model the terrestrial TR device, we must now consider the amount of thermal radiation from the sky incident on the earth's surface. Outside of the atmospheric transparency window, the sky's emission resembles that of a blackbody at the ambient air temperature. Within the window, though the upper levels of the atmosphere are transparent to LWIR, these wavelengths are absorbed and emitted by water molecules present in varying concentrations throughout the troposphere, the lowest level of the atmosphere, in the form of humidity, fog, and, most notably, cloud cover. Thermal emission from clouds depends on the optical depth and altitude; optically thick clouds have high emission, and optically thin clouds, typically at higher altitudes and colder temperatures, have lower emission.²¹ Therefore, the earth's cooling power, which is the difference between the outgoing radiation and the downwelling power, and the performance of a terrestrial TR cell rely on local weather conditions; optimal conditions would be clear skies and low humidity. At 300 K ambient temperature, broadband cooling powers of 160 W/m^2 and $>120 \text{ W/m}^2$ have been estimated^{22,23} and measured,⁶ respectively. In general, without detailed sky emission measurements, we can use the cooling powers to extract an effective sky temperature that simulates real sky conditions. To do this, we first define the cooling power as the difference in power emitted from a blackbody at 300 K and one at T_a and then use Planck's law to solve for T_a . To calculate extractable electrical power, we follow the principles of detailed balance and use eq 3, this time with an ideal broadband cell emissivity of $\varepsilon = 1$ for wavelengths greater than $3 \mu\text{m}$ and $\varepsilon = 0$ elsewhere, simulating a perfect solar reflector (or transmitter) and IR emitter. We find that under the real sky conditions measured in Colorado, that is, a broadband cooling power of 130 W/m^2 at 300 K ambient,⁶ which corresponds to an effective sky temperature of 276 K, an ideal broadband TR cell held at the ambient 300 K and pointed at the sky has a power output $>2 \text{ W/m}^2$. This number increases to 3.2 W/m^2 if we use the predicted maximum net cooling rate of 160 W/m^2 for 300 K ambient, corresponding to an effective sky temperature of 270 K, achievable under optimal weather conditions. Figure 2 highlights the maximum extractable power for broadband coupling with selected effective sky temperatures that simulate different conditions: the ideal deep space (no atmosphere) at 3 K, clear sky conditions (no clouds and low humidity) at 270 K, and a humid suburban sky at 290 K. This last effective sky temperature (290 K) was chosen by using a lower cooling power of 60 W/m^2 , which is consistent with inserting overcast weather conditions into the modified Swinbank model for downwelling IR and computing an effective sky temperature according to Stefan's law.^{24,25}

To more accurately estimate power production, further detailed sky emission information is required. Terrestrial measurements of downwelling atmospheric LWIR are not common, however, 24 h averages of approximately 35 W/m^2 in the winter and 75 W/m^2 in the summer, with respective surface temperatures of 285 and 300 K, between $8\text{--}13 \mu\text{m}$ have been reported at the ARM Climate Research Facility in Lamont, OK.²⁶ Multiplying eq 1 by photon energy and this time integrating over the transparency window, these power measurements correspond to blackbodies of $T_a = 223$ and 262

K, which we can use as T_a in eq 3 to simulate the incident radiation on the device. To calculate extractable power, we again apply the principles of detailed balance, and, restricting cell emissivity such that $\varepsilon_{\text{LWIR}} = 1$ and $\varepsilon = 0$ outside the ATW, we calculate an extractable power in Lamont, OK of 3.2 and 1.6 W/m^2 in the winter and summer, respectively. In these cases, the net cooling power within the window is approximately 80 W/m^2 . If the estimated max cooling power of 140 W/m^2 within the ATW is assumed,²³ a 300 K cell could potentially extract up to 10 W/m^2 by accessing the atmospheric transparency window alone. In this case, when we restrict emission to the window using a selective emitter, the maximum power is achieved using a material of bandgap $E_g = 0.095 \text{ eV}$. We note that, under any terrestrial configuration, the TR device is not coupling directly with deep space, but rather with the atmosphere. Because sky emission and the effective sky temperature fluctuate significantly with weather conditions and the optimal bandgap increases with effective sky temperature, optimization of a TR cell will depend on the environmental conditions (e.g., cloud cover, humidity, ground temperature, etc.) under which the cell will be operating. Much like a conventional solar cell, the power conversion ability of a TR device is dramatically reduced by cloud cover.

Up to this point in the discussion, we have considered only the radiative generation-recombination processes for creating or removing electron-hole pairs that are not collected through current extraction. We complete the analysis by discussing the effects of nonradiative generation and recombination. Auger recombination (and the inverse process of impact ionization) is considered the dominant nonradiative process in low bandgap semiconductors, especially near room temperature.²⁷ To account for this process, eq 3 is modified to include a nonradiative generation term, \dot{N}_{NR} , such that the total power output is

$$P = JV = qV[\dot{N}(T_a, 0) - \dot{N}(T_c, qV) + \dot{N}_{\text{NR}}] \quad (4a)$$

While \dot{N}_{NR} would be a function of voltage for an actual p - n device, we have suppressed this dependence to focus on the fraction of nonradiatively generated carriers by defining the nonradiative generation ratio

$$\eta \equiv \frac{\dot{N}_{\text{NR}}}{\dot{N}(T_a, 0) + \dot{N}_{\text{NR}}} \quad (4b)$$

such that the total power output becomes

$$P = qV \left[\left(\frac{1}{1 - \eta} \right) \dot{N}(T_a, 0) - \dot{N}(T_c, qV) \right] \quad (4c)$$

Figure 6 shows how the extractable power decreases as nonradiative generation/recombination rates increase for a cell operating under realistic weather conditions, that is, an effective sky temperature of 270 K.

Next, we consider what levels of nonradiative generation/recombination can be expected in real devices. Tennant showed that reverse-bias leakage currents in experimental IR photodetectors follow an exponential trend, called the "Rule 07," that increases with decreasing bandgap and increasing device temperature.^{27,28} Comparing this exponential fit to the calculated radiative current densities of our TR device, it appears that nonradiative processes would outweigh the radiative ones by a factor of up to 10^4 in the optimal bandgap regime of $\sim 0.04 \text{ eV}$, and up to 10^3 for $E_g \sim 0.1 \text{ eV}$. However,

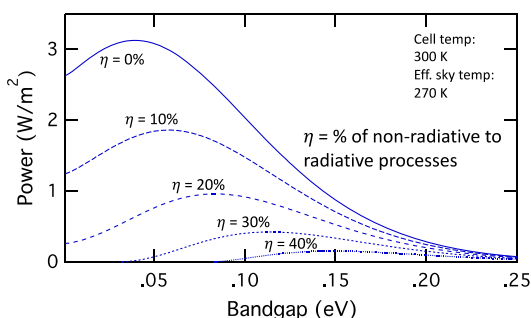


Figure 6. Power output for different percentages of nonradiative generation, η , for a thermoradiative device operating at 300 K exposed to a sky with effective temperature of 270 K, simulating clear sky conditions.^{22,23}

the previously mentioned experiment performed by Santhanam and Fan showed an extractable power that corresponds to a nonradiative generation percentage of 3%, in accordance with the above treatment, compared to $\eta \sim 99\%$, as predicted with Rule 07. This result suggests that although nonradiative processes are present in these materials, they may not significantly inhibit the development of TR devices. Additionally, regarding device improvement, significant Auger suppression has been demonstrated in low-gap semiconductors under strong reverse bias.²⁹ However, our operating voltage is around $1 k_B T$, so new material developments, such as quantum wells, which predict a suppression of the Auger mechanism by 2 orders of magnitude,³⁰ may be useful in order to keep the nonradiative generation rate low. Compared to bulk materials, the room-temperature Auger recombination coefficients of type-II InAs-Ga_{1-x}In_xSb-InAs-AlSb quantum well lasers ($E_g \sim 0.28$ eV) and InAs/GaSb superlattice photoconductors ($E_g \sim 0.1$ eV) have been reduced by a factor of 4³¹ and 8,³² respectively, through appropriate engineering. These experimental results lead to the conclusion that a well-designed TR device, built purely with existing materials and engineering methods, such as the InAs/GaSb superlattice, could conceivably produce 1.5 W/m^2 in the broadband configuration or

potentially up to 8.4 W/m^2 with selective emission under the night sky.

■ INTEGRATION, MATERIALS, AND SCALABILITY

The underlying functionality of the TR cell relies on maintaining the temperature difference between the cell and the sky. As with any radiating body facing a colder environment, the cell loses energy as it emits, so in order to maintain the cell temperature, it must be in thermal contact with the earth. Further, the top surface of the cell must be optically coupled to the sky. These criteria thus suggest a module that (i) is thermally conducting on the bottom surface, which can include a back-reflector to direct the cell's radiation toward the sky, (ii) is encapsulated to protect the cell from the environment and restrict conductive and convective heat loss, and (iii) includes an infrared window on the front to allow radiative heat transfer to the sky.

For the active material, there are several possible low bandgap semiconductors that could serve as starting points for investigation. InSb can reach a bandgap below 0.1 eV,³³ which can be useful in proof of principle devices. However, for optimal power, even lower bandgaps are needed. Hg_{1-x}Cd_xTe, a heavily characterized material used in the infrared sensing industry, can be bandgap engineered into the realm needed for a high-power-producing TR cell with a Cd composition of around $x = 0.1$.³⁴ Newer materials that can have even lower bandgaps, such as graphene-hBN heterostructures, could also prove useful in a TR device. Although difficult to fabricate, it has been shown that alternately stacking sheets of graphene with hBN can open a bandgap of 0.04 eV in the graphene layer,³⁵⁻³⁷ which would be an excellent bandgap for a nighttime PV cell. However, any chosen material may likely need additional engineering in order to suppress nonradiative generation/recombination.

If the cell can be constructed to operate at higher temperatures, it could generate even more power, as shown in Figure 5b. Notably, if sunlight is used to heat the cell up to 330 K, the maximum power increases to 13.3 W/m^2 for a 270 K effective sky temperature. If connected to an external heat

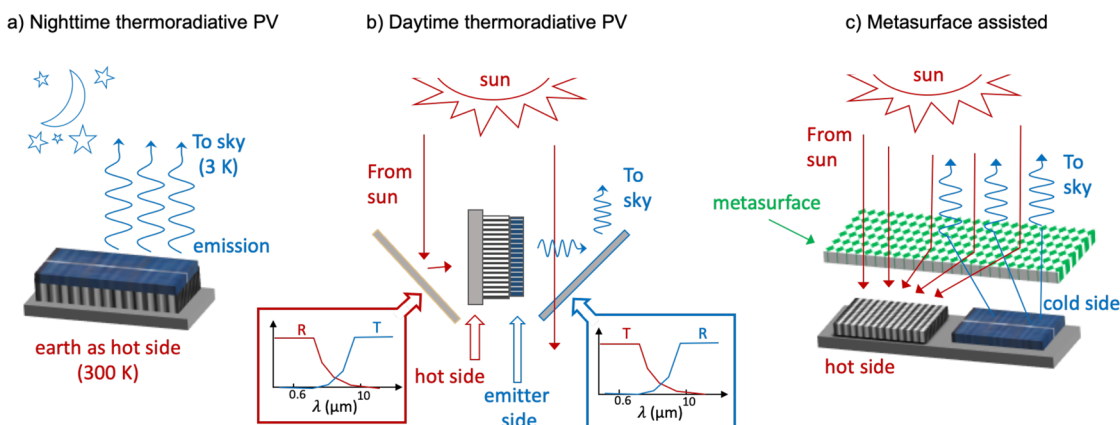


Figure 7. Conceptual designs for thermoradiative cell configurations. (a) The basic design, assumed throughout the calculations in this paper, includes a “hot side” that is in thermal contact with earth, while the top of the cell can radiate thermal power to deep space. (b) Rotating the cell and using spectrally selective optical reflectors, we can heat up the “hot side” of the cell during the day to enhance power generation. A mirror that reflects the sun’s irradiance toward the cell heats one side while a corresponding mirror transmits the solar irradiance and reflects the thermal emission from the cell toward deep space. In this configuration, a selective solar absorber, a material with high solar absorbance and low thermal emittance,³⁸ could be used as the cell’s hot side. (c) This effect could also be performed more compactly using metamaterials. A metamaterial can be engineered to direct solar irradiance passing through it toward one side of the device while directing thermal radiation from the cell back toward deep space, allowing for a planar cell design where one-half is for heating and the other is for thermal emission.

source (or concentrated solar) and operating at $T_c = 471$ K, the maximum power reaches 200 W/m^2 . Additionally, these higher operating temperatures allow for greater power generation at larger bandgaps. At an operating temperature of 443 K, a material with a bandgap of 0.1 eV could produce 100 W/m^2 . At this temperature, InSb, with $E_g = 0.17$, could directly produce 40 W/m^2 without additional bandgap engineering. Possible configurations for such devices are sketched in Figure 7. Further, instead of using the sun as a heat source, one can also envision attaching these devices to industrial exhaust systems, consistently at high temperatures, and pointing them toward the sky, in order to extract additional power from the wasted heat of the industrial process. Alternatively, instead of competing with traditional PV for power production, a nighttime PV module could be coupled with existing PV in order to maximize the 24 h power cycle. In open, arid environments, where solar farms are already common, the effective sky temperature is low enough to provide for near-ideal TR power production. If a retractable nighttime PV unit were rolled out on top of the standard solar modules after sunset, a solar farm could produce an additional 12% more electricity.

In conclusion, as the global push toward carbon neutrality continues, the sun is not the only sky-facing option for power generation. Thermoradiative photovoltaic devices offer the possibility of nighttime power generation by optically coupling with the cold of deep space (or the cool atmosphere). Such devices need strong absorption and emission at thermal wavelengths and clear and dry conditions to facilitate optical access to the night sky. Deep space offers an intriguing low-temperature thermal sink that has the potential to help provide electrical power at night and day through the clever use of photonics, optics, and materials science.

AUTHOR INFORMATION

Corresponding Author

*E-mail: jnmunday@ucdavis.edu.

ORCID

Jeremy N. Munday: [0000-0002-0881-9876](https://orcid.org/0000-0002-0881-9876)

Author Contributions

J.N.M. conceived and supervised the project. T.J.D. performed the calculations. All authors discussed the results and contributed to the manuscript preparation.

Notes

The authors declare no competing financial interest.

ACKNOWLEDGMENTS

The authors thank the Munday Lab group members and colleagues in IREAP for stimulating discussion throughout the preparation of this work. T.J.D. acknowledges a University of Maryland Clark Fellowship.

REFERENCES

- (1) Shockley, W.; Queisser, H. J. Detailed Balance Limit of Efficiency of P-n Junction Solar Cells. *J. Appl. Phys.* **1961**, *32*, 510–519.
- (2) Strandberg, R. Theoretical Efficiency Limits for Thermoradiative Energy Conversion. *J. Appl. Phys.* **2015**, *117*, 055105.
- (3) National Renewable Energy Laboratory. U.S. State Solar Resource Maps, <https://www.nrel.gov/gis/solar.html> (accessed Jun 27, 2019).
- (4) Bahadori, M. N. Passive Cooling Systems in Iranian Architecture. *Sci. Am.* **1978**, *238*, 144–154.

- (5) Raman, A. P.; Anoma, M. A.; Zhu, L.; Rephaeli, E.; Fan, S. Passive Radiative Cooling below Ambient Air Temperature under Direct Sunlight. *Nature* **2014**, *515*, 540–544.

- (6) Zhai, Y.; Ma, Y.; David, S. N.; Zhao, D.; Lou, R.; Tan, G.; Yang, R.; Yin, X. Scalable-Manufactured Randomized Glass-Polymer Hybrid Metamaterial for Daytime Radiative Cooling. *Science* **2017**, *355*, 1062–1066.

- (7) Atiganyanun, S.; Plumley, J. B.; Han, S. J.; Hsu, K.; Cytrynbaum, J.; Peng, T. L.; Han, S. M.; Han, S. E. Effective Radiative Cooling by Paint-Format Microsphere-Based Photonic Random Media. *ACS Photonics* **2018**, *5*, 1181–1187.

- (8) Mandal, J.; Fu, Y.; Overvig, A.; Jia, M.; Sun, K.; Shi, N.; Zhou, H.; Xiao, X.; Yu, N.; Yang, Y. Hierarchically Porous Polymer Coatings for Highly Efficient Passive Daytime Radiative Cooling. *Science* **2018**, *362*, 315–319.

- (9) Zhu, L.; Raman, A. P.; Fan, S. Radiative Cooling of Solar Absorbers Using a Visibly Transparent Photonic Crystal Thermal Blackbody. *Proc. Natl. Acad. Sci. U. S. A.* **2015**, *112*, 12282–12287.

- (10) Safi, T. S.; Munday, J. N. Improving Photovoltaic Performance through Radiative Cooling in Both Terrestrial and Extraterrestrial Environments. *Opt. Express* **2015**, *23*, A1120–A1128.

- (11) Lin, C.; Wang, B.; Teo, K. H.; Zhang, Z. Performance Comparison Between Photovoltaic and Thermoradiative Devices. *J. Appl. Phys.* **2017**, *122*, 243103.

- (12) Zhang, X.; Peng, W.; Lin, J.; Chen, X.; Chen, J. Parametric Design Criteria of an Updated Thermoradiative Cell Operating at Optimal States. *J. Appl. Phys.* **2017**, *122*, 174505.

- (13) Hsu, W. C.; Tong, J. K.; Liao, B.; Huang, Y.; Boriskina, S. V.; Chen, G. Entropic and Near-Field Improvements of Thermoradiative Cells. *Sci. Rep.* **2016**, *6*, 34837.

- (14) Santhanam, P.; Fan, S. Thermal-to-Electrical Energy Conversion by Diodes under Negative Illumination. *Phys. Rev. B: Condens. Matter Mater. Phys.* **2016**, *93*, 161410.

- (15) Würfel, P. Thermodynamic Limitations to Solar Energy Conversion. *Phys. E* **2002**, *14*, 18–26.

- (16) Munday, J. N. Tackling Climate Change through Radiative Cooling. *Joule* **2019**, *3*, 2057.

- (17) Cool Roof Rating Council. Rated Products Directory, <https://coolroofs.org/directory> (accessed Jul 12, 2019).

- (18) Yu, N.; Mandal, J.; Overvig, A.; Shi, N. N. Systems and Methods for Radiative Cooling and Heating. WO2016205717A1, December 22, 2016.

- (19) Grenier, P. Réfrigération Radiative. Effet de Serre Inverse. *Rev. Phys. Appl.* **1979**, *14*, 87–90.

- (20) Gentle, A. R.; Smith, G. B. Radiative Heat Pumping from the Earth Using Surface Phonon Resonant Nanoparticles. *Nano Lett.* **2010**, *10*, 373–379.

- (21) Nugent, P. W.; Shaw, J. a.; Piazzolla, S. Infrared Cloud Imager Development for Atmospheric Optical Communication Characterization, and Measurements at the JPL Table Mountain Facility. *IPN Prog. Rep.* **2013**, *42*, 1–31.

- (22) Sun, X.; Sun, Y.; Zhou, Z.; Alam, M. A.; Bermel, P. Radiative Sky Cooling: Fundamental physics, materials, structures, and applications. *Nanophotonics* **2017**, *6*, 997–1015.

- (23) Zhao, D.; Aili, A.; Zhai, Y.; Xu, S.; Tan, G.; Yin, X.; Yang, R. Radiative sky cooling: Fundamental principles, materials, and applications. *Appl. Phys. Rev.* **2019**, *6*, 021306.

- (24) Goforth, M. A.; Gilchrist, G. W.; Sirianni, J. D. Cloud Effects on Thermal Downwelling Sky Radiance. *Proc. SPIE* **2002**, *4710*, 203–213.

- (25) Pandey, D. K.; Lee, R. B.; Paden, J. Effects of Atmospheric Emissivity on Clear Sky Temperatures. *Atmos. Environ.* **1995**, *29*, 2201–2204.

- (26) Byrnes, S. J.; Blanchard, R.; Capasso, F. Harvesting Renewable Energy from Earth's Mid Infrared Emissions. *Proc. Natl. Acad. Sci. U. S. A.* **2014**, *111*, 3927–3932.

- (27) Tennant, W. E. Rule 07th Revisited: Still a Good Heuristic Predictor of p/n HgCdTe Photodiode Performance? *J. Electron. Mater.* **2010**, *39*, 1030–1035.

(28) Teherani, J. T.; Agarwal, S.; Chern, W.; Solomon, P. M.; Yablonovitch, E.; Antoniadis, D. A. Auger Generation as an Intrinsic Limit to Tunneling Field-Effect Transistor Performance. *J. Appl. Phys.* **2016**, *120*, 084507.

(29) Emelie, P. Y.; Phillips, J.; Velicu, S.; Wijewarnasuriya, P. S. Parameter Extraction of HgCdTe Infrared Photodiodes Exhibiting Auger Suppression. *J. Phys. D: Appl. Phys.* **2009**, *42*, 234003.

(30) Chiu, L.; Yariv, A. Auger Recombination in Quantum-Well InGaAsP Heterostructure Lasers. *IEEE J. Quantum Electron.* **1982**, *18*, 1406–1409.

(31) Felix, C. L.; Meyer, J. R.; Vurgaftman, I.; Lin, C. H.; Murry, S. J.; Zhang, D.; Pei, S. S. High-Temperature 4.5-Mm Type-II Quantum-Well Laser with Auger Suppression. *IEEE Photonics Technol. Lett.* **1997**, *9*, 734–736.

(32) Mohseni, H.; Litvinov, V.; Razeghi, M. Interface-Induced Suppression of the Auger Recombination in Type-II InAs/GaSb Superlattices. *Phys. Rev. B: Condens. Matter Mater. Phys.* **1998**, *58*, 15378–15380.

(33) Jin, Y. J.; Tang, X. H.; Ke, C.; Yu, S. Y.; Zhang, D. H. Bandgap Engineering of InSb by N Incorporation by Metal-Organic Chemical Vapor Deposition. *J. Alloys Compd.* **2018**, *756*, 134–138.

(34) Norton, P. HgCdTe Infrared Detectors. *Opto-Electron. Rev.* **2002**, *10*, 159–174.

(35) Cassabois, G.; Valvin, P.; Gil, B. Hexagonal Boron Nitride Is an Indirect Bandgap Semiconductor. *Nat. Photonics* **2016**, *10*, 262–266.

(36) Ramasubramaniam, A.; Naveh, D.; Towe, E. Tunable Band Gaps in Bilayer Graphene-BN Heterostructures. *Nano Lett.* **2011**, *11*, 1070–1075.

(37) Song, X.; Sun, J.; Qi, Y.; Gao, T.; Zhang, Y.; Liu, Z. Graphene/*h*-BN Heterostructures: Recent Advances in Controllable Preparation and Functional Applications. *Adv. Energy Mater.* **2016**, *6*, 1600541.

(38) Kennedy, C. E. Review of Mid-to High-Temperature Solar Selective Absorber Materials. NREL/TP-520–31267; OSTI: Oak Ridge, TN, 2002.